

σ -Silane Platinum(II) Complexes as Intermediates in C–Si Bond Coupling Processes

Pablo Ríos,^[a] Hugo Fouilloux,^[a] Josefina Díez,^[b] Pietro Vidossich,^[c,d] Agustí Lledós^{[c]*} and Salvador Conejero^{*[a]}

This work is dedicated to Prof. Pablo Espinet on the occasion of his 70th birthday celebration

Abstract: Platinum complexes [Pt(NHC')(NHC)][BAR^F] (NHC' denotes the cyclometallated N-heterocyclic carbene ligand, NHC) react with primary silanes RSiH₃ leading to the cyclometallated platinum(II) silyl complexes [Pt(NHC-SiHR')(NHC)][BAR^F] through a process that involves the formation of C–Si and Pt–Si bonds with concomitant extrusion of H₂. Low temperature NMR studies indicate that the process proceeds with the initial formation of the σ -SiH complexes [Pt(NHC')(NHC)(HSiH₂R)][BAR^F] which are stable at temperatures below 0 °C. At higher temperatures activation of one Si–H bond followed by a C–Si coupling reaction generates an agostic SiH platinum hydride derivative [Pt(H)(NHC'-SiH₂R)(NHC)][BAR^F] that undergoes a second SiH bond activation producing the final products. Computational modelling of the reaction mechanism indicate that the stereochemistry of the silyl/hydride ligands after the first Si–H bond cleavage dictates the nature of the products, favoring the formation of a C–Si bond over C–H, in contrast to previous results observed with tertiary silanes. Furthermore, the process involves a *trans* to *cis* isomerization of the NHC ligands before the second Si–H bond cleavage.

Introduction

Construction of carbon-silicon bonds is a powerful method for the functionalisation of organic molecules.^[1] Hydrosilylation reactions of alkenes and alkynes are probably the most efficient methods to this aim,^[2] but there is an increasing interest in dehydrocoupling processes of silanes and hydrocarbons, both aromatic and aliphatic, as alternative to produce this type of bonds.^[3] Besides, this methodology has proven to be very useful in the design of silyl ligands through post-functionalization reactions within the coordination sphere at a metal center.^[4] In spite of the knowledge gathered over the years, mechanistic studies related to the formation of C–Si bonds are rather

uncommon. In particular, the occurrence of σ -SiH complexes during the reaction turned to be elusive to prove.^[5]

Recently, we have been able to isolate and detect cationic Pt(II) σ -SiH species [Pt(HSiR₃)(NHC')(NHC)][BAR^F] (where NHC represents an N-heterocyclic carbene ligand and NHC' its cyclometallated form) using tertiary silanes, HSiR₃ (R = Et, Ph; NHC = 1-(*tert*-butyl)-3-isopropylimidazol-2-ylidene, *t*Bu¹Pr) or secondary silanes (NHC = 1,3-di-*tert*-butylimidazol-2-ylidene, *t*Bu) (Scheme 1).^[6] These compounds exhibit an unusual η^1 -SiH coordination mode^[7] as the most stable arrangement, but can adopt a η^2 -SiH mode with low energy barriers. In fact, these species are only stable in solution at temperatures below 0 °C, undergoing cleavage of the Si–H bond at higher temperatures generating the 14-electron Pt(II) silyl species [Pt(SiR₃)(NHC)₂][BAR^F] (Scheme 1). This process involves the cleavage of Pt–C and Si–H bonds with concomitant formation of Pt–Si and C–H bonds. No products derived from the alternative process, that is formation of Pt–H and C–Si bonds, were detected. Nevertheless, it is not always evident which of the different coupling products can be formed. For example, Milstein et al. reported that addition of silanes to platinum(II) methyl complexes can lead to methane and a platinum-silyl derivative, or to C–Si reductive coupling species and a Pt–H complex, or mixtures containing all of the possible coupling products.^[5h,8] The effect of the electronic nature of the substituents on the silane has been investigated in iridium systems and found to be a key factor in directing the reactivity towards C–H or C–Si bonds, with electron withdrawing substituents favouring the former.^[9]

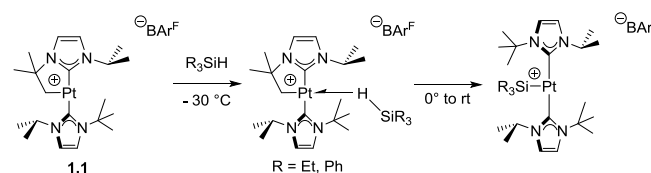
In this article we have explored the reactivity of cyclometallated Pt(II) complexes [Pt(NHC')(NHC)][BAR^F] towards primary silanes. At variance with tertiary silanes, the reaction leads, under very mild conditions (rt), to a double Si–H bond activation process involving the selective formation of C–Si–Pt bonds. Low temperature NMR studies together with DFT calculations provided valuable mechanistic insights that implicate transient σ -SiH and agostic SiH Pt(II) complexes before releasing a molecule of H₂.

[a] P. Ríos, H. Fouilloux, Dr. S. Conejero
Instituto de Investigaciones Químicas (IIQ), Departamento de Química Inorgánica, Centro de Innovación en Química Avanzada (ORFEO-CINCA)
CSIC and Universidad de Sevilla.
C/ Américo Vespucio 49, 41092 Sevilla, Spain
E-mail: sconejero@iiq.csic.es

[b] Dr. J. Díez
Laboratorio de Compuestos Organometálicos y Catálisis (Unidad asociada al CSIC), Departamento de Química Orgánica e Inorgánica, Universidad de Oviedo, C/ Julián Clavería 8, 33008, Oviedo, Spain

[c] Dr. P. Vidossich, Prof. Dr. A. Lledós
Departament de Química -Centre de Innovació en Química Avanzada (ORFEO-CINCA)
Universitat Autònoma de Barcelona
Campus UAB, 08193 Cerdanyola del Vallès, Spain
E-mail: agusti@klingon.uab.es

[d] COBO Computational Bio-Organic Chemistry Bogotá, Department of Chemistry, Universidad de los Andes, Carrera 1 #18A-12, 111711 Bogotá, Colombia.

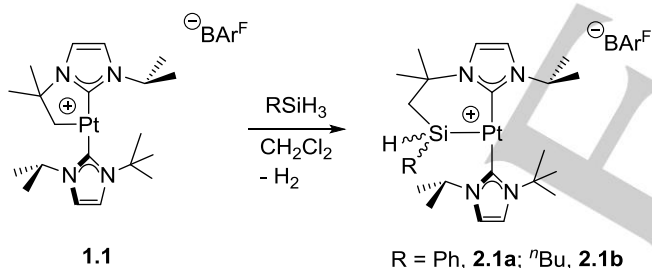


Scheme 1. Reaction of complex **1.1** with tertiary silanes.

Results and Discussion

Reactions of primary silanes with cyclometallated complexes [Pt(NHC')(NHC)][BAR^F]

The reaction of platinum(II) complex **1.1** (see ESI for details about the numbering used in this article) with primary silanes H₃SiR (R = ⁿBu, Ph) in CD₂Cl₂ at rt (Scheme 2) is characterised by gas evolution (H₂; signal detected at 4.64 ppm in the ¹H NMR spectrum) and the formation of a new species defined by a non-symmetric nature of the N-heterocyclic carbene ligands according to ¹H and ¹³C{¹H} spectra. In particular, the most characteristic feature of the ¹H NMR spectrum is the observation of two distinct CH(CH₃)₂ methinic protons and four signals for the =CH imidazole protons, in a similar way than the cyclometallated starting complex **1.1**. Most significantly, resonances at 4.04 and 3.52 with a relative integral of one for **2.1a** and **2.1b**, respectively, exhibiting large coupling to ¹⁹⁵Pt of ca. 120 Hz have been attributed to the Si–H group.^[10] This latter resonances correlate with signals at -10.8 ppm (**2.1a**, ¹J_{Pt,Si} ~1500 Hz) and -1.5 ppm (**2.1b**) in the ¹H,²⁹Si HMQC NMR spectra, in the expected region for silyl platinum complexes.^[6b,10] This information, together with the fact that H₂ is extruded from the system, suggest that the silyl-cyclometallated Pt(II) complexes **2.1a** and **2.1b** have been formed (Scheme 2). No traces of the silyl species arising from C–H coupling have been detected, contrary to the results observed in the reaction of **1.1** with tertiary silanes (Scheme 1).



Scheme 2. Reaction of complex **1.1** with primary silanes leading to the silyl-cyclometallated species **2.1**.

The identity of **2.1a** was confirmed by X-ray crystallography (Figure 1). Complex **2.1a** crystallises with a molecule of methylene chloride which is in close proximity to the metal centre (Pt...Cl bond distance 2.8026(1) Å).^[11] As expected from the NMR data the platinum atom is bonded to one ^tBuⁱPr ligand and a silyl fragment linked to the second ^tBuⁱPr ligand through a CH₂ moiety. The Pt–Si bond distance (2.2693(1) Å) is similar to that found in related systems.^[6b,10] The six-membered ring of the metallacycle is in a boat conformation enforcing the NHC ligand to form an angle of ca 54.1° with respect to the coordination plane around the platinum atom, and to be almost coplanar to the non-metallated NHC (angle defined by the planes of the two imidazole rings: 17.9°).

The construction of C–Si bonds is not limited to the platinum complex **1.1**. The related platinum complexes

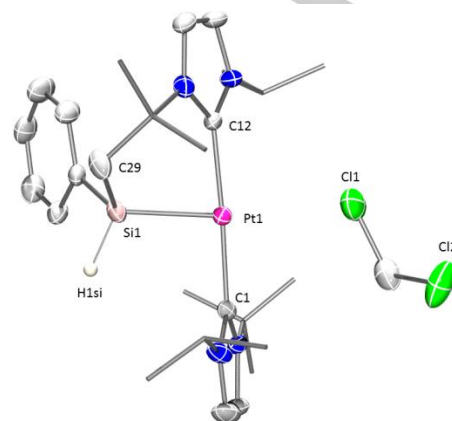
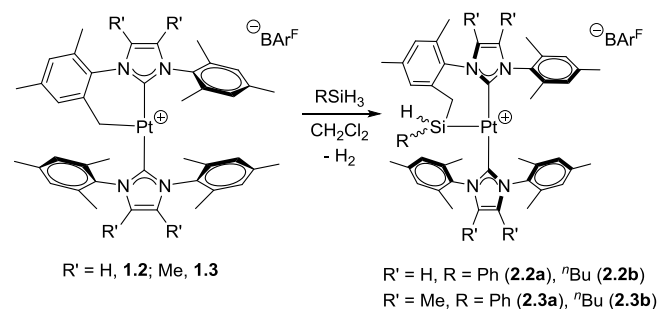


Figure 1. Solid-state structure of complex **2.1a**. Thermal ellipsoids for selected atoms are drawn at the 50% probability level; hydrogen atoms (except H1si) and the anion is omitted for clarity. Selected bond distances (Å) and angles (°): Pt1–Si1, 2.2693(1); Pt1–C1, 2.039(1), Pt1–C12, 2.036(4), Si1–C29, 1.889(5); C1–Pt1–Si1, 96.20(12), C12–Pt1–Si1, 81.11(12); C29–Si1–Pt1, 107.07(16), C1–Pt1–C12, 177.29(16).

[Pt(IMes')(IMes)][BAR^F], **1.2**, (IMes = 1,3-dimesitylimidazol-2-ylidene) and [Pt(IMes*)(IMes*)(BAR^F)]⁺, **1.3**, (IMes* = 1,3-dimesityl-4,5-dimethylimidazol-2-ylidene) react very fast with primary silanes RSiH₃ (R = Ph, ⁿBu) at rt to generate the corresponding silyl-cyclometallated complexes **2.2** and **2.3** (Scheme 3). As for **1.1**, the reaction induces the release of H₂ and both the ¹H and ¹³C{¹H} NMR evinced the highly unsymmetrical nature of the new complexes (see ESI). In the ¹H NMR spectra of complexes **2.2-3a** and **2.2-3b**, the Si–H proton resonates at ca. 3.6 and 2.9 ppm, respectively, as doublets (³J_{H,H} = 6.9 Hz (**2.2a**), 6.5 (**2.3a**)) and triplets (³J_{H,H} = 6.3 Hz (**2.2b**), 6.5 Hz (**2.3b**)) due to coupling to the CH₂–Si unit. Furthermore, these signals show a large coupling to ¹⁹⁵Pt (²J_{Pt,H}



Scheme 3. Reaction of complexes **1.2** and **1.3** with primary silanes leading to the silyl-cyclometallated species **2.2** and **2.3**.

= 165 Hz, **2.2a**; ²J_{Pt,H} = 168 Hz, **2.3a**; ²J_{Pt,H} = 160 Hz, **2.2b**; ²J_{Pt,H} = 165 Hz, **2.3b**). These resonances correlate in the ¹H,²⁹Si HMQC NMR spectra with signals at -0.5 (**2.2a**), -1.6 (**2.3a**), 9.0

(**2.2b**) and 7.9 (**2.3b**) ppm. The different chemical shifts for the silyl groups in the ^{29}Si NMR spectra with respect to complexes **2.1a** and **2.1b** (between 8-10 ppm) are attributed to the different ligand strain of the two metallacycles and the different electronic properties of the NHC ligands.

Formation of complex **2.3b** is accompanied by minor amounts (ca. 5-7%) of the symmetrical silyl complex $[\text{Pt}(\text{SiH}_2^t\text{Bu})(\text{IMes}^*)_2][\text{BAR}^F]$, **4.3b** (see below).^[12]

Bright yellow crystals suitable for X-ray diffraction studies for complexes **2.2a** and **2.2b** were grown by slow diffusion of concentrated solutions of the complexes in CH_2Cl_2 into pentane (Figure 2). The platinum atom in the two molecules is tri-

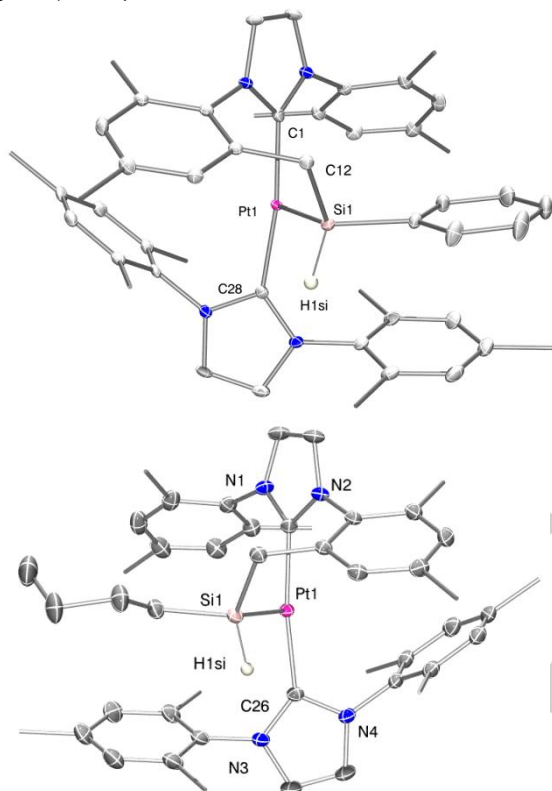


Figure 2. Solid-state structure of complex **2.2a** and **2.2b**. Thermal ellipsoids for selected atoms are drawn at the 30% probability level; hydrogen atoms (except H1si) and the anion is omitted for clarity. Selected bond distances (Å) and angles (°): **2.2a**: Pt1–Si1, 2.2609(8); Pt1–C1, 2.017(3); Pt1–C28, 2.026(3); Si1–C12, 1.890(3); C1–Pt1–Si1, 90.25(8); C28–Pt1–Si1, 94.24(8); C1–Pt1–C28, 171.85(11). **2.2b**: Pt1–Si1, 2.2619(6); Pt1–C1, 2.013(2); Pt1–C26, 2.021(2); Si1–C19, 1.894(2); C1–Pt1–Si1, 89.42(6); C26–Pt1–Si1, 95.76(7); C1–Pt1–C26, 172.37(9).

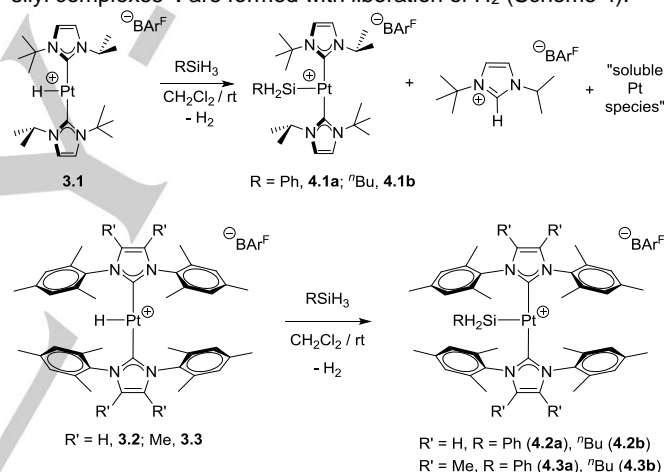
coordinated. At variance with complex **2.1a**, no methylene chloride is present in the structures and no diagnostic Pt–C or Pt–H bond distances for agostic interactions with the methyl groups of the mesityl fragments are apparent (the closest $\text{Pt}\cdots\text{H}\cdots\text{C}$ contacts appear at 2.756 and 3.519(2) Å, for **2.2a**, and 3.035 and 3.751(2) Å for **2.2b**).^[13] Thus, both systems can be considered as 14-electron Pt(II) species.^[14] The structures clearly show the new C–Si and Pt–Si bonds formed, with a bond

distance in the latter being nearly identical to that in **2.1a** (2.2609(8) and 2.2619(6) for **2.2a** and **2.2b**, respectively). The seven-membered metallacycle is in a boat conformation, as previously observed in cobalt and iron systems reported by Deng.^[4b,e,f] All these compounds are very stable both in solution and in the solid state, even under air.

The reactions shown above are processes that take place under very mild reaction conditions, that contrast with previous observations in related Pt(II) complexes (usually requiring heating to induce the C–Si bond coupling process).^[5h] Likely, the vacant site in the platinum–NHC systems reduce the energy barrier for the coupling process (usually, dissociation of one of the ligands is a prerequisite for coupling processes).

Reactions of primary silanes with platinum hydride complexes $[\text{Pt}(\text{H})(\text{NHC})_2][\text{BAR}^F]$

If, on the other hand, the reaction of the primary silanes is carried out with the platinum hydrides $[\text{Pt}(\text{H})(\text{NHC})_2][\text{BAR}^F]$ (**3**) a different outcome of the reactions is observed. In this case, the silyl complexes **4** are formed with liberation of H_2 (Scheme 4).



Scheme 4. Reaction of hydride complexes **3** with primary silanes leading to silyl complexes **4**.

No products arising from C–Si coupling processes have been detected, even after allowing the solutions to stand in solution for several hours, indicating that these silyl derivatives are not intermediates *en route* to complexes **2** (through C–H bond activation processes followed by reductive C–Si bond coupling). Although very clean reactions are observed using as starting material complexes **3.2** and **3.3**, reactions of the silanes with **3.1** result in partial decomposition leading to the imidazolium salt $t\text{Bu}^i\text{Pr}\text{-HBAr}^F$ (ca. 12% for **4.1a** and 20% for **4.1b**) together with other soluble platinum species of unknown composition, precluding purification of complexes **4.1** (Scheme 4).

Reactions of the primary silanes with platinum hydrides **3.2** and **3.3** are slightly slower than those with the corresponding cyclometallated species **1.2** and **1.3**, requiring about 10 min for

completion. However, whereas the reaction of **3.1** with PhSiH_3 is rather fast (less than 5 min) the process needs ca. 2 h with $^t\text{BuSiH}_3$. Likely, this effect is due to the easiness of activation of Si-H bonds of silanes bearing more electron-withdrawing groups (phenyl in the present case) due to a more efficient pi-back-donation of the metal to the σ^* orbital of the Si-H bond.^[6a]

In all complexes **4**, characterisation is straightforward by NMR spectroscopy. At variance with cyclometallated silyl complexes **2**, only one set of signals are observed for the two N-heterocyclic carbenes ligands (see ESI). Evidence for the formation of the Pt-Si bond arises from the large coupling of SiH protons to ^{195}Pt (100 to 115 Hz). These signals resonate between 2.01 to 3.77 ppm with a relative integral value of two. At the same time they correlate in the $^1\text{H},^{29}\text{Si}$ HMQC NMR spectra with signals at -38.1 to -34.3 ppm (complexes **4**.[**1-3**]a) and -28.5 to -24.2 ppm (complexes **4**.[**1-3**]b), considerably up-field shifted with respect to the corresponding chemical shifts found for complexes **2.1-3**.

All these compounds are very stable both in solution and in the solid state, even under air. They do not undergo Pt-Si cleavage under heating (through cyclometallation processes) nor upon pressurizing with H_2 (4 atm), their solutions remaining unaltered. This is in agreement with the known strength of the Pt-Si bond.^[15]

Yellow crystals suitable for X-ray diffraction studies were grown for complex **4.2a** (Figure 3). The structure of the cation features the expected *trans* arrangement of the two NHC ligands with the third coordination site occupied by the silyl ligand. The two NHC ligands are tilted with respect to the coordination plane around the platinum centre, but forming considerably different angles of 76.9 and 40.3°, to minimise steric repulsions between the mesityl rings. The Pt-Si bond distance of 2.2703(9) Å is

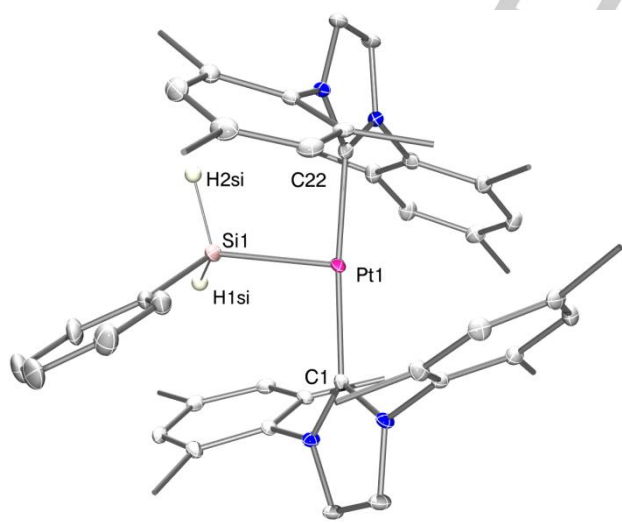


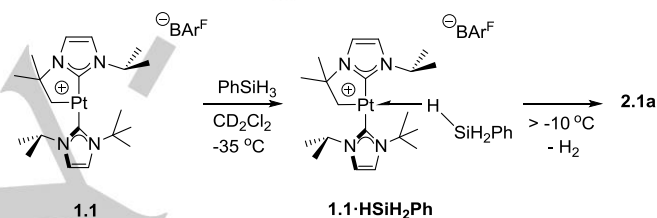
Figure 3. Solid-state structure of complex **4.2a**. Thermal ellipsoids for selected atoms are drawn at the 30% probability level; hydrogen atoms (except H1si) and the anion is omitted for clarity. Selected bond distances (Å) and angles (°): Pt1-Si1, 2.2703(9); Pt1-C1, 2.028(3), Pt1-C22, 2.010(3); C1-Pt1-Si1, 98.51(9), C22-Pt1-Si1, 86.63(9); C1-Pt1-C22, 174.78(12).

nearly identical (within experimental error) to that observed in complexes **2.2a** and **2.2b**. Once more the closest CH group to the metal centre is too far to consider any agostic interaction (Pt...H bond distance, 2.88 Å; Pt...C bond distance, 3.54 Å).

Low-Temperature NMR studies

In previous work,^[6] we reported that σ -SiH complexes can be observed (and in some cases isolated) by NMR at temperatures below 0 °C. In order to determine if the same type of complexes can be detected with the less hindered primary silanes and to look for possible reaction intermediates in the processes leading to C-Si bonds, low temperature NMR studies have been carried out.

We first analysed the reaction of derivative $[\text{Pt}(\text{tBuPr})(\text{tBuPr})][\text{BAR}^F]$, **1.1**, with PhSiH_3 in CD_2Cl_2 at -35 °C. At this temperature a clean reaction takes place leading to a new species that according to ^1H , $^{13}\text{C}\{^1\text{H}\}$ and ^{29}Si NMR spectra is consistent to its formulation as the σ -SiH complex **1.1-HSiH₂Ph** (Scheme 5). The ^1H NMR shows a signal in the



Scheme 5. Schematic representation of the reaction of complex **1.1** with primary silane PhSiH_3 at low temperature.

hydride region (-4.79 ppm) with a relative integral of one, exhibiting coupling to ^{195}Pt ($^1J_{\text{Pt,H}} = 435$ Hz) and ^{29}Si ($^1J_{\text{Si,H}} = 75$ Hz) (Figure 4). The former coupling constant is slightly higher than that observed for the related complex

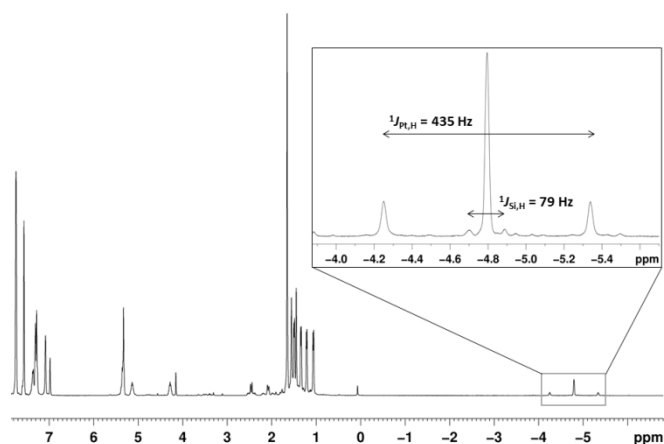
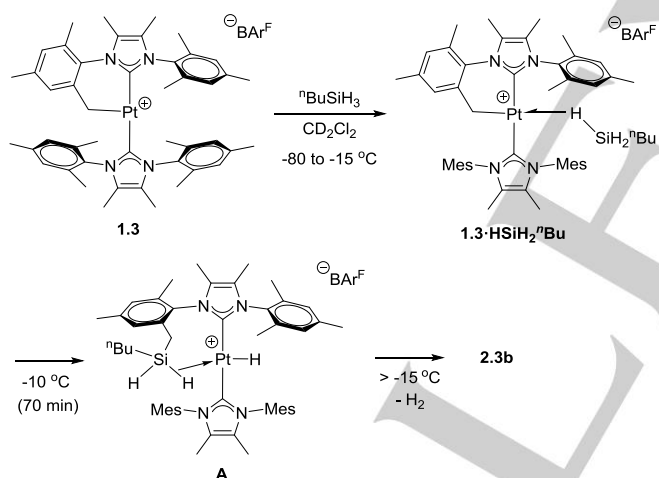


Figure 4. Low T (-35 °C) NMR spectra of complex **1.1-HSiH₂Ph**.

[Pt(HSiEt₃)(^tBuPr')(ⁱBuPr)][BAR^F], **1.1-HSiEt₃**, (¹J_{Pt,H} = 396 Hz)^[6a], whereas the coupling to ²⁹Si is only slightly smaller (79 Hz). This signal, attributed to the bridging Pt...H...Si proton, correlates in the ¹H,²⁹Si HMQC NMR spectrum with a signal at -51.8 ppm. Another resonance in the ¹H NMR at ca. 5.35 ppm (partially masked by the residual CDHCl₂) also correlates with the peak at -51.8. This signal, whose integral value is approximately 2, corresponds to the terminal SiH₂ protons. The Pt-CH₂ protons resonate as two doublets centred at 2.46 and 2.08 ppm (²J_{H,H} = 12 Hz) exhibiting coupling to ¹⁹⁵Pt of 53 and 85 Hz, which are considerably smaller than those found in precursor **1.1**, suggesting the presence of a coordinating ligand (ⁿBuSiH₃) in *trans*.^[14] As the temperature is allowed to increase (from -10 °C to -5 °C), some new intermediate species can be observed in the ¹H NMR, some of which contain broad signals in the hydride region. However, these species coexist with the σ-SiH complex and with the final product **2.1a**, which starts appearing at the same range of temperatures, hampering the identification of the hydride species. Finally, at 5 °C all starting material is fully converted into the cyclometallated silyl complex **2.1a** with concurrent formation of H₂ (observed at 4.64 ppm).

The reaction of the cyclometallated complex **1.3** and ⁿBuSiH₃ was also studied by low temperature NMR allowing the identification of some intermediate species (Scheme 6). Once more, the first complex observed at temperatures between -80 °C and -15 °C was the silane σ-SiH complex **1.3-HSiH₂ⁿBu**



Scheme 6. Schematic representation of the reaction products observed at low temperature in the reaction of complex **1.3** with primary silane ⁿBuSiH₃.^[16]

(together with a small portion of the hydride complex **3.3-HSiH₂ⁿBu**, see below).^[12] The bridging Pt...H...Si proton resonates as a doublet (²J_{H,H} = 3.0 Hz) at -7.98 ppm with coupling constants to ¹⁹⁵Pt and ²⁹Si of 500 and 67 Hz, respectively. The terminal SiH protons appear as multiplets at 3.95 (t) and 3.18 (td) ppm. All the SiH protons show a correlation in the ¹H,²⁹Si HMQC NMR spectrum with a signal at ca. -53.5 ppm (-59.0 ppm for the free ⁿBuSiH₃ at the same temperature). At temperatures above -15 °C a new complex starts appearing, which after warming to -10 °C for 70 min is the major product observed in the NMR spectrum (Figure 5). The most significant

feature of the ¹H NMR is a signal in the hydride region at -5.9 ppm, with a ¹J_{Pt,H} of 990 Hz and a relative integral of 2. According to a NOESY experiment, this signal is exchanging with another proton that resonates as a broad signal at ca. 4.0 ppm (relative integral value of 1), which indicate a rapid exchange, on the NMR time scale, of the SiH protons and the Pt-H.

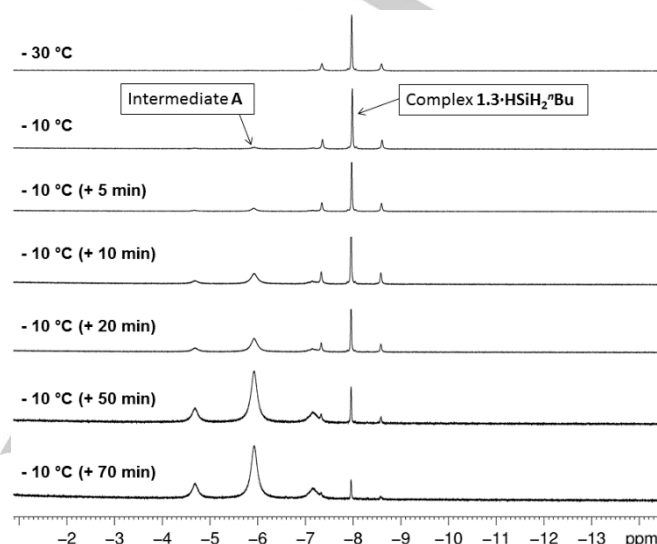


Figure 5. ¹H NMR (hydride region) showing the evolution of complex **1.3-HSiH₂ⁿBu** to intermediate **A** at -10 °C.

Unfortunately, attempts to observe a correlation of these signals in the ¹H,²⁹Si HMQC NMR spectrum for this intermediate were unsuccessful at this temperature. The rest of the NMR signals in the ¹H NMR were too complex to establish the structure of this intermediate. However, based on DFT calculations (see below), this intermediate is likely the agostic SiH platinum hydride complex **A** (Scheme 6). In fact, upon cooling down the sample to -80 °C the signal at -5.9 ppm splits into two new resonances at -4.74 and -6.88 ppm with two distinct couplings to ¹⁹⁵Pt of ca. 380 Hz and 1580 Hz, respectively (Figure 6). These signals are likely those of the agostic SiH (-4.74 ppm) and the Pt-H (-6.88 ppm)

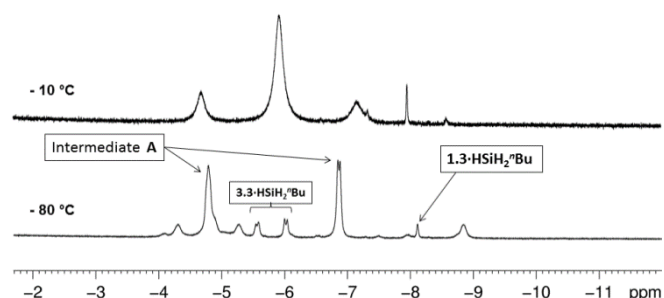
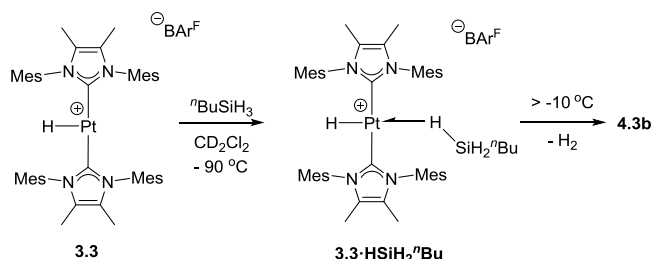


Figure 6. VT ¹H NMR spectra of intermediate **A** (hydride region). At -80 °C a small portion of complex **3.3-HSiH₂ⁿBu** is observed.

protons. The ^1H , ^{29}Si HMQC NMR spectrum shows a correlation of the ^1H signals at -4.74 ppm and 3.97 ppm (relative integral of 1) with a signal at -21.0 ppm, which is consistent with a secondary silane. Upon warming up the solution to rt, complex **2.3a** is finally formed together with H_2 .

To further clarify the nature of compound **A**, a low temperature NMR experiment was performed for the reaction of platinum hydride $[\text{Pt}(\text{H})(\text{IMes}^*)_2][\text{BAR}^{\text{F}}]$, **3.3**, and butylsilane (Scheme 7). At -90 °C a new complex, identified as the σ -SiH derivative **3.3-HSiH $_2$ ^nBu** , is cleanly formed for which the



Scheme 7. Low temperature reaction of complex **3.3** with $^n\text{BuSiH}_3$ leading to the σ -SiH intermediate **3.3-HSiH $_2$ ^nBu** and its evolution at temperatures above -10 °C.

resonances in the hydride region serve as a model for those observed in intermediate **A**. Significantly, the chemical shifts for the bridging SiH and the Pt-H protons resonate as two different signals at δ -5.55 (d, $^2J_{\text{H,H}} = 17$ Hz, $^1J_{\text{Pt,H}} = 423$ Hz) and -6.08 (d, $^2J_{\text{H,H}} = 17$ Hz, $^1J_{\text{Pt,H}} = 1544$ Hz) (Figure 7). A third broad signal, with a relative integral of 2, appears at 3.71 ppm attributed to the terminal SiH $_2$ protons. All these signals show exchange in NOESY experiments, but only those at 3.71 ppm and -5.55 exhibit cross peaks in the ^1H , ^{29}Si HMQC NMR spectrum with a signal at -49.8 ppm. The chemical shifts and coupling constants to ^{195}Pt detected in the ^1H NMR for complex **3.3-HSiH $_2$ ^nBu** are comparable to those attributed to intermediate **A**, thus providing

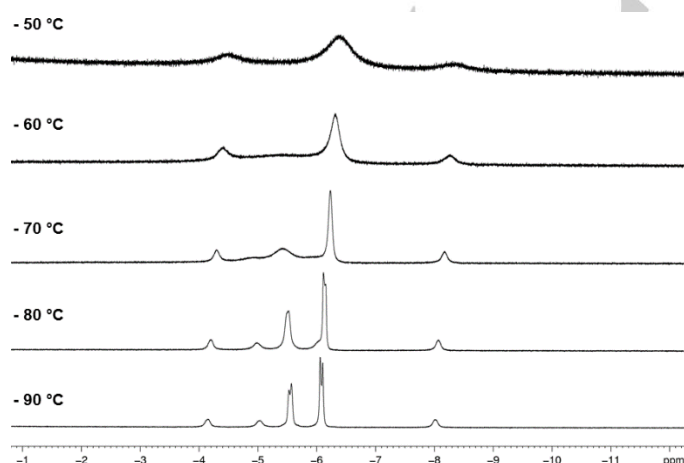


Figure 7. VT ^1H NMR of complex **3.3-HSiH $_2$ ^nBu** (hydride region).

evidence for the structure suggested in Scheme 6. The two signals in the hydride region merge into a broad one at -50 °C, exhibiting coalescence at -30 °C. At temperatures above -10 °C the silyl complex **4.3b** starts appearing being the only observable complex at rt.

Reaction mechanism for the C-Si bond coupling: structures and energies

We have performed DFT calculations with the M06 functional to pinpoint the reaction mechanism of the C-Si bond coupling process and to analyse the origin of the preference of C-Si over C-H bond formation (Computational Details in the ESI).

The Gibbs energy profile of the most likely pathway for the formation of the C-Si coupling product **2.2b** starting from $[\text{Pt}(\text{IMes}^*)(\text{IMes})]^+$ (**1.2**) and $^n\text{BuSiH}_3$ is depicted in Figure 8. Alternative routes explored entailing higher barriers are collected in the ESI. The reaction starts with the formation of the σ -complex **1.2-HSiH $_2$ ^nBu** , from which a formally Si-H oxidative addition (see below) yields, after crossing the transition state **1.2-TS_Si-H**, an unstable silyl-hydride intermediate **11**. This intermediate has a square pyramidal geometry, with the silyl ligand in the apical position. In this intermediate the silicon atom is close to the cyclometallated carbon atom to which it couples, with geometrical parameters consistent with the presence of an attractive Si-C interaction ($\text{Si}\cdots\text{C} = 2.46$ Å, $\text{Si-Pt-C} = 63.6^\circ$). The Si-C bond forms (**12**) almost barrierless (**1.2-TS_Si-C**). Intermediate **12** is a T-shaped 14-electron complex. The vacant position *trans* to the hydride ligand is filled by an agostic η^2 -Si-H interaction with the dangling silyl group, resulting in a stable, potentially detectable, intermediate (**12b**). Indeed, intermediate **12b** can be correlated with the species **A**, observed spectroscopically (NMR) at low temperature in the reaction of $[\text{Pt}(\text{IMes}^*)(\text{IMes})]^+$ (**1.3**) with $^n\text{BuSiH}_3$ (Scheme 6). Therefore, the agostic SiH-platinum hydride **12b** is a key species along the transformation of σ -silane complexes into the silyl-cyclometallated Pt(II) complexes.

The reaction advances with a second Si-H bond activation and formation of H_2 . However, a *trans*-NHC to *cis*-NHC isomerization is required to end up with the Pt-Si-C coupled product **2.2b**. If the last step of the reaction occurs through the *trans*-NHC arrangement the barrier for the Si-H bond breaking/H-H forming step (29.6 kcal mol $^{-1}$) is higher than that of the C-H coupling pathway (27.4 kcal mol $^{-1}$), therefore directing the reaction toward the 14-electron Pt(II) silyl product (See ESI). In the *trans* isomer **12b** the η^2 -Si-H bond is *trans* to the hydride ligand, and the two H atoms that must couple to form H_2 are far away and essentially *trans* ($\text{H}\cdots\text{H} = 3.44$ Å, $\text{H}_{\text{bridging}}\text{-Pt-H} = 172.4^\circ$). The corresponding transition state has a *cis*-dihydride nature ($\text{H}_{\text{bridging}}\cdots\text{H} = 2.03$ Å, $\text{H}_{\text{bridging}}\text{-Pt-H} = 78.8^\circ$), with a hydride *trans* to the strong donor silyl ligand, thus raising notably the energy of the transition state.

The isomerisation of the agostic SiH *trans*-NHC platinum hydride **12b** to the *cis* (**cis-12b**) takes place through transition state **12b-TS_t-c** in which the agostic Si-H interaction is absent. The Gibbs energy barrier for the isomerization (21.9 kcal mol $^{-1}$)

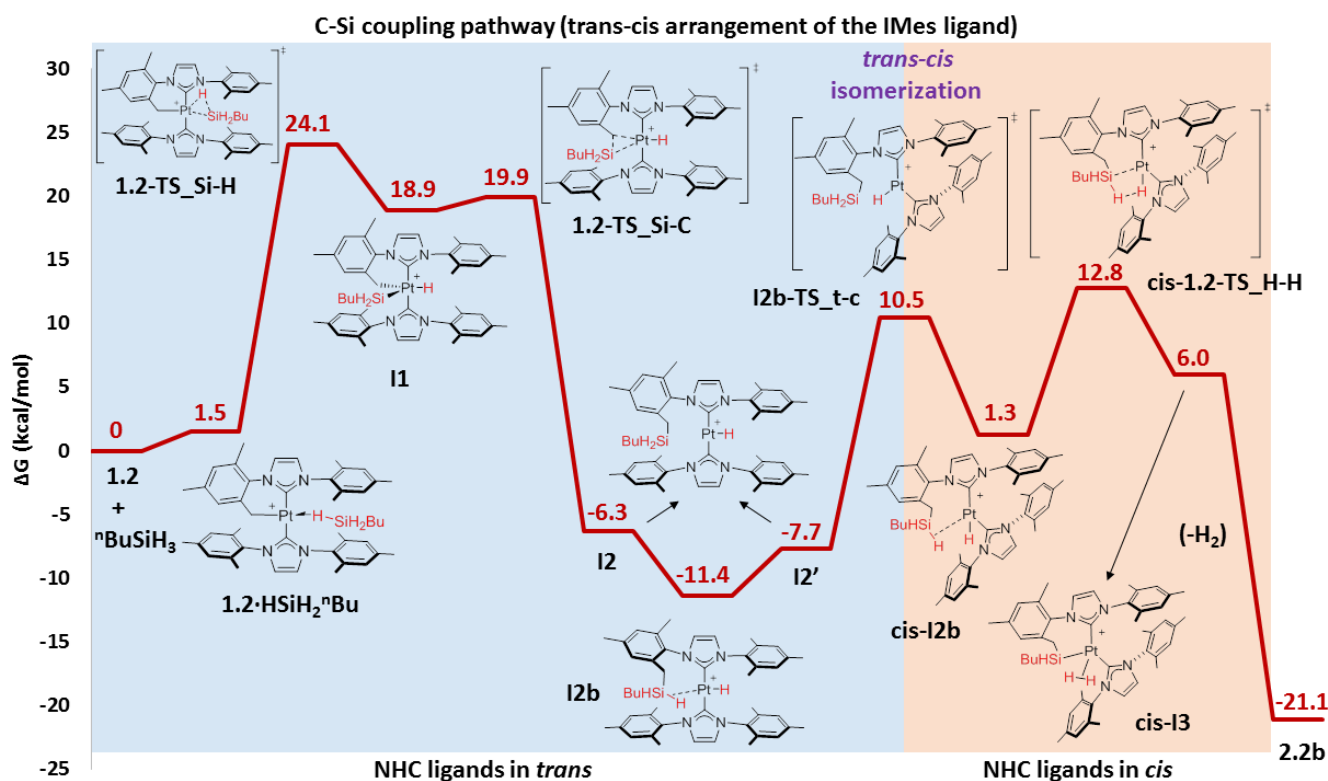


Figure 8. Favoured Gibbs energy profile in DCM for the reaction of complex **1.2** with $n\text{BuSiH}_3$. Relative Gibbs energies at 298.15K in kcal mol $^{-1}$.

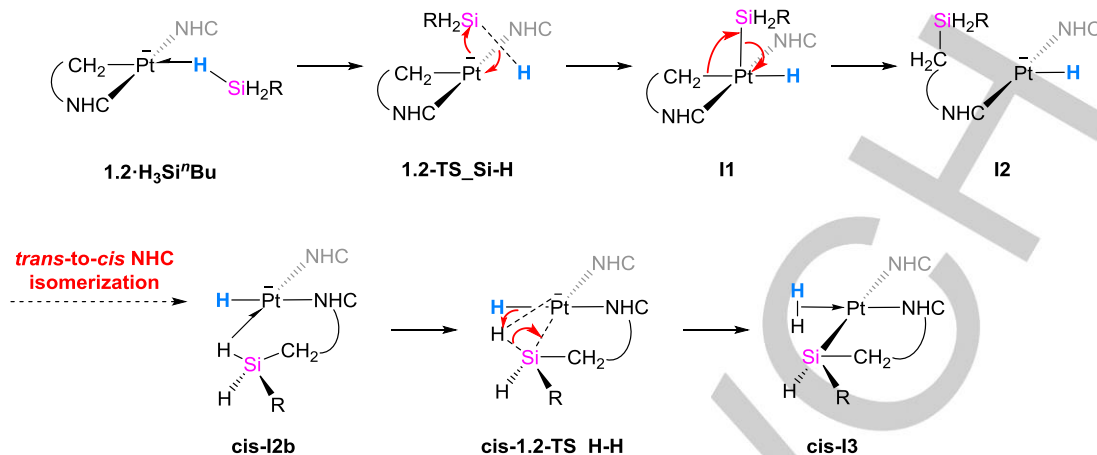
is lower than that of the first Si–H bond activation (24.2 kcal mol $^{-1}$). A stronger SiH agostic interaction is present in **cis-I2b** (Si–H_{bridging} = 1.72 Å, Pt–H_{bridging} = 1.65 Å) making the Si–H bond prone to break. Indeed, the coordination of the silicon group is close to a η^2 -SiH mode (Si...Pt = 2.52 Å, Si–H–Pt = 96.9°), in which the H_{bridging} should have a marked hydride character. In this intermediate the two H atoms that couple are already mutually *cis* (H...H = 2.30 Å, H_{bridging}–Pt–H = 90.3°), allowing a σ -CAM mechanism^[17] in which a hydrido- η^2 (Si–H) σ -complex transforms into a silyl- η^2 (H–H) σ -complex.^[18] From intermediate **cis-I2b** formation of a coordinated H₂ molecule takes place by means of a σ -CAM mechanism^[17] with a barrier of only 11.5 kcal mol $^{-1}$ (**cis-1.2-TS_H-H** with H...H = 1.34 Å). The complex restores the *trans* arrangements of the NHC ligands when releasing the H₂ molecule from **cis-I3** to yield the final product **2.2b**. The alternative “all-*cis*” pathway, in which a *trans* to *cis* isomerisation of the NHC ligands takes place before the formation of the silane σ -complex features a higher barrier (24.6 kcal mol $^{-1}$, see ESI) and it does not account for the formation of a stable intermediate (**I2b**) as experimentally observed.

In the last step of the reaction a silyl complex is formed with liberation of H₂ from a platinum hydride and an η^2 -Si–H bond. This reaction has been experimentally studied with primary silanes (see Scheme 4). To ascertain the requirement of the *trans* to *cis* isomerization of the NHC ligands in the H₂ formation step we have also computationally studied the reaction of the platinum hydride [Pt(H)(I^tBuPr)₂]⁺ (**3.1**) with $n\text{BuSiH}_3$ to form the

silyl complex **4.1b**, with liberation of H₂ (Scheme 4), assuming both *trans*- and *cis*-arrangement of the NHC ligands. The reaction involves a barrier of 35.2 kcal mol $^{-1}$ in the *trans* isomer and 20.0 kcal mol $^{-1}$ in the *cis* isomers. The *trans* to *cis*-NHC isomerization of **3.1** has a barrier of 16.8 kcal mol $^{-1}$ and gives a *cis* isomer 8.8 kcal mol $^{-1}$ above the initial *trans*-NHC complex **3.1** (see ESI). As a further evidence of the flexibility of the NHC–Pt–NHC angle in these tricoordinated [HPt(NHC)₂]⁺ complexes, we have found that the formation of the imidazolium salt decomposition product (Scheme 4) takes place with a transition state in which the NHC–Pt–NHC angle has closed to 134° (ESI).

Electronic analysis of the reaction mechanism

We have used a localised orbital approach to analyse the electronic rearrangements taking place along the reaction mechanism.^[19] In this approach, that we have already applied to other organometallic reactions,^[20] Kohn–Sham orbitals are transformed into maximally localised orbitals (LMOs), and the centroids of these LMOs are computed in selected structures along the reaction path. The movement of the localised orbital centroids along the reaction path gives information about the electron rearrangements of the bond-breaking and forming processes. In this manner an arrow pushing scheme of the reaction of primary silanes with cyclometallated [Pt(NHC')(NHC)]⁺ complexes can be obtained from the DFT



Scheme 8. Electronic rearrangements in the reaction of cyclometallated $[\text{Pt}(\text{NHC})(\text{NHC})]^+$ complexes with primary silanes to yield the C–Si coupled product.

calculations. Scheme 8 summarizes this analysis; a detailed account of the calculations can be found in the ESI.

Starting from the σ -complex **1.2-H₃SiⁱBu**, the first Si–H bond activation (**1.2-TS_{Si-H}**) features an electron pair from platinum moving towards silicon to form the Pt–Si bond, while the electron pair of the Si–H bond moves to form the Pt–H bond, thus reaching **I1**. Next, the C–Si bond is formed by the electron pair of the Pt–C bond of the cyclometallated ligand. At the same time, the electron pair of the Pt–Si bond goes back to platinum, giving the 14-electron intermediate **I2**, which is further stabilised by an agostic $\text{Pt}\cdots\eta^2(\text{Si-H})$ interaction. The *trans*- to *cis*-NHC isomerization prepares the system (**cis-I2b**) for the second Si–H bond activation and H₂ formation. In this last step (**cis-1.2-TS_{H-H}**) the electron pair of the Si–H bond moves towards Pt to form the Pt–Si bond and the electron pair of the Pt–H bond moves to pick up the proton. A lone pair from Pt assists the proton transfer (see ESI). This four-center electronic rearrangement allows the direct H-transfer from the σ -bond H–Si ligand to the hydride with no change in the oxidation state of the metal, characteristic of σ -CAM mechanisms.^[17,18]

The first step of the reaction (Si–H bond activation) is formally an oxidative addition, which displays interesting stereoelectronic features. The stereoselectivity of this formal oxidative addition at Pt determines the nature of the products: if the Si–H bond breaks to give the H in apical position, C–H bond coupling will follow, else if the Si occupies the apical position, a C–Si bond will form. In both cases, transition states with square-pyramidal structures are involved. The important point is that, in both cases, the ligand at the apical position has a cationic character (either a silylium ion or a proton). To illustrate this feature, we have used the localised orbital analysis commented above, using the position of the localised orbital centroid along the bond axis as an estimator of bond polarity (see ESI).^[21] As shown in Figure 9 and ESI, the nature of the Pt–Si and Pt–H bonds depends on whether the bond is apical or equatorial (in the plane of the other Pt ligands). Comparing **1.2-TS_{C-H}** and

1.2-TS_{Si-H}, we may appreciate that the centroid of the localised Pt–H bond is closer to the H atom when the bond is equatorial (a hydride ligand; b) in Figure 9) compared to when the bond is apical (a proton ligand; a) in Figure 9). Similarly, the centroid of the localised Pt–Si bond is closer to the Si atom when the bond is equatorial (a silyl ligand; a) in Figure 9) than when it is axial (a silylium ligand; b) in Figure 9). This formally silylium ion is easily added to the cyclometallated carbon atom, forming in this way the C–Si bond.

The nature of silyl ligands is a matter of discussion. A recent study of the energetic and electronic features of metal–silyl interactions has revealed that, in several complexes silyl groups can be Z-ligands, thus behaving as metal-bound “silylium” ions, $[\text{SiR}_3]^+$.^[22] There are a number of experimental and computational reports showing that square-planar Pt(II) complexes can act as hydrogen bond acceptors through its d_{z^2} orbital directed perpendicularly to the PtL_4 plane.^[23] Neutron diffraction studies of the platinum complex $\text{trans-}[\text{PtCl}_2(\text{NH}_3)(\text{N-glycine})]\cdot\text{H}_2\text{O}$, showed that a water molecule points its hydrogen towards the axial position of the platinum center.^[24] Our computational analysis of the C–H bond activation step in the Shilov process led us to formulate the transient intermediate $\text{PtHCl}_2(\text{H}_2\text{O})(\text{CH}_3)$, with a formally apical hydride ligand, as a Pt(II) species, ready to transfer a proton to the bulk solution in the following step.^[25] The present study revealed that the RSiH_2 moiety has silylium character when in apical position, which is crucial for its reactivity toward the formation of C–Si bonds.

Conclusions

In summary, we have reported that primary silanes can form σ -SiH complexes with cationic electron deficient Pt(II) complexes, $[\text{Pt}(\text{NHC})(\text{NHC})]^+$. These compounds evolve at room temperature through a double Si–H bond activation process that involves the formation of C–Si and Si–Pt bonds

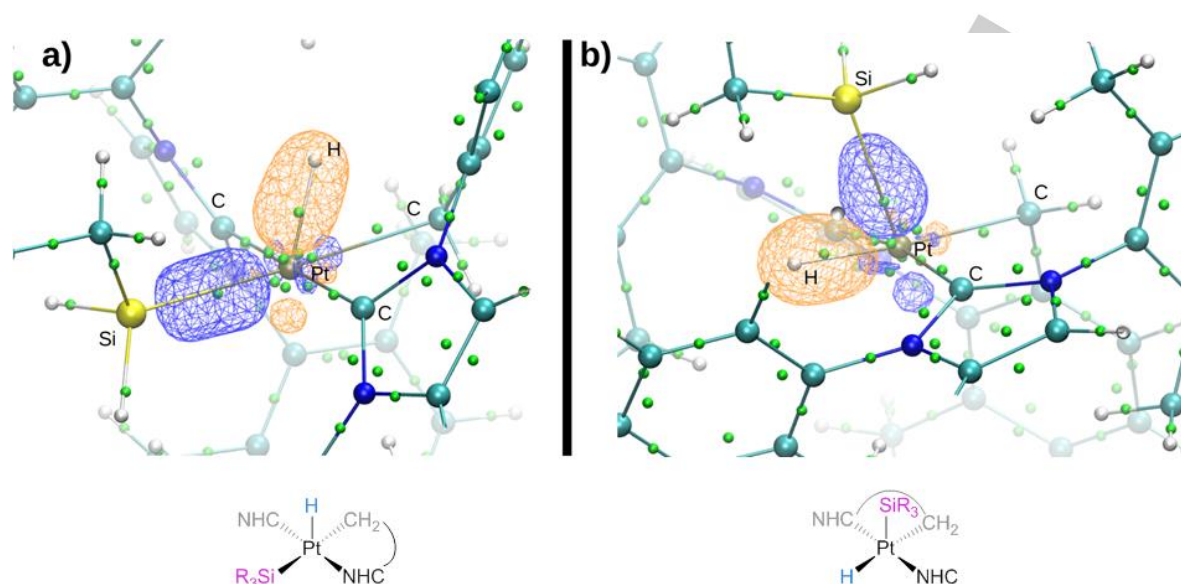


Figure 9. Localised orbital analysis of a) **1.2-TS_C-H** (see Figure S47 in the ESI) and b) **1.2-TS_Si-H**. C atoms are shown as cyan spheres, Si in yellow, H in white, Pt in gray and localized orbital centroids as small green spheres. Isosurfaces of the localized orbitals corresponding to the Pt–Si (blue surface) and Pt–H (orange surface) are also shown.

with concomitant extrusion of H₂. These results contrast with the reactivity observed for tertiary silanes, for which a C–H coupling process leading to platinum silyl species [Pt(SiR₃)(NHC)₂]⁺ is preferred after Si–H bond activation. DFT calculations in combination with low temperature NMR studies provided a mechanistic picture of the process that involves a *trans* to *cis* isomerisation of the NHC ligands after the first Si–H bond activation as a more favourable pathway, highlighting the importance of a “flexible” coordination geometry around the metal centre. Interestingly, a localised orbital analysis revealed an enhanced silylium character of the silicon atom when the silyl fragment is located at the apical position that likely favours the C–Si coupling event.

Acknowledgements

Financial support (FEDER contribution) from the MINECO (Projects CTQ2016-76267-P, CTQ2017-87889-P and CTQ2016-81797-REDC) and the Junta de Andalucía (Project FQM-2126) is gratefully acknowledged. P.R. thanks the Junta de Andalucía for a research grant.

Conflicts of interest

The authors declare no conflict of interest.

Keywords: carbene ligands • Density functional calculations • Platinum • Si ligands • silanes

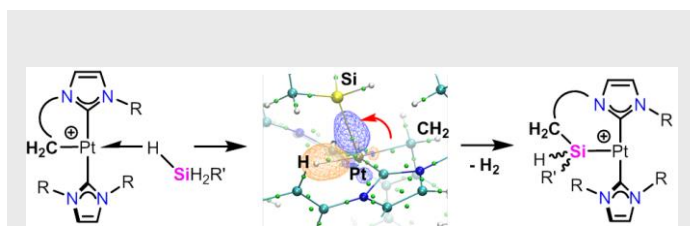
- [1] T. Komiyama, Y. Minami, T. Hiyama, *ACS Catal.* **2017**, *7*, 631–651.
- [2] a) X. Du, Z. Huang, *ACS Catal.* **2017**, *7*, 1227–1243; b) M. Oestreich, *Angew. Chem. Int. Ed.* **2016**, *55*, 494–499; c) J. Sun, L. Deng, *ACS Catal.* **2016**, *6*, 290–300; d) B. Marciniak, H. Maciejewski, C. Pietraszuk, P. Pawluć, *Hydrosilylation: A Comprehensive Review of Recent Advances*, Springer, **2009**; e) A. K. Roy, *Adv. Organomet. Chem.* **2008**, *55*, 1–59.
- [3] a) C. Cheng, J. F. Hartwig, *Chem. Rev.* **2015**, *115*, 8946–8975; b) Z. Xu, W.-S. Huang, J. Zhanga, L.-W. Xu, *Synthesis* **2015**, *47*, 3645–3668.
- [4] a) C. A. Cuevas-Chávez, J. Zamora-Moreno, M. A. Muñoz-Hernández, C. Bijani, S. Sabo-Etienne, V. Montiel-Palma, *Organometallics* **2018**, *37*, 720–728; b) J. Sun, L. Luo, Y. Luo, L. Deng, *Angew. Chem. Int. Ed.* **2017**, *56*, 2720–2724; c) J. Sun, C. Ou, C. Wang, M. Uchiyama, L. Deng, *Organometallics* **2015**, *34*, 1546–1551; d) Z. Mo, L. Deng, *Synlett* **2014**, *25*, 1045–1049; e) O. Ouyang, L. Deng, *Organometallics* **2013**, *32*, 7268–7271; f) Z. Mo, Y. Liu, L. Deng, *Angew. Chem. Int. Ed.* **2013**, *52*, 10845–10849.
- [5] a) T. Lee, J. F. Hartwig, *J. Am. Chem. Soc.* **2017**, *139*, 4879–4886; b) L. Rubio-Pérez, M. Iglesias, J. Munárriz, V. Polo, V. Passarelli, J. J. Pérez-Torrente, L. A. Oro, *Chem. Sci.* **2017**, *8*, 4811–4822; c) C. Cheng, J. F. Hartwig, *J. Am. Chem. Soc.* **2014**, *136*, 12064–12072; d) G. Choi, H. Tsurugi, K. Mashima, *J. Am. Chem. Soc.* **2013**, *135*, 13149–13161; e) D. Zhu, D. J. Kozera, K. D. Enns, P. H. M. Budzelaar, *Angew. Chem. Int. Ed.* **2012**, *51*, 12211–12214; f) M. E. Fasulo, E. Calimano, J. M. Buchanan, T. D. Tilley, *Organometallics* **2013**, *32*, 1016–1028; g) F. Ozawa, T. Tani, H. Katayama, *Organometallics* **2005**, *24*, 2511–2515; h) M. E. van der Boom, J. Ott, D. Milstein, *Organometallics* **1998**, *17*, 4263–4266.

- [6] a) P. Ríos, H. Fouilloux, P. Vidossich, J. Díez, A. Lledós, S. Conejero, *Angew. Chem. Int. Ed.* **2018**, *57*, 3217–3221; b) P. Ríos, J. Díez, J. López-Serrano, A. Rodríguez, S. Conejero, *Chem. Eur. J.* **2016**, *22*, 16791–16795.
- [7] a) J. Chen, E. Y.-X. Chen, *Angew. Chem. Int. Ed.* **2015**, *54*, 6842–6846; b) A. Y. Houghton, J. Hurmalainen, A. Mansikkamäki, W. E. Piers, H. M. Tuononen, *Nat. Chem.* **2014**, *6*, 983–988; c) J. Yang, P. S. White, C. K. Schauer, M. Brookhart, *Angew. Chem. Int. Ed.* **2008**, *47*, 4141–4143; d) S. P. Hoffmann, T. Kato, F. S. Tham, C. A. Reed, *Chem. Commun.* **2006**, 767–769.
- [8] R. Goikhman, M. Aizenberg, L. J. W. Shimon, D. Milstein, *J. Am. Chem. Soc.* **1996**, *118*, 10894–10895.
- [9] a) M. Aizenberg, D. Milstein, *J. Am. Chem. Soc.* **1995**, *117*, 6456–6464; b) M. Aizenberg, D. Milstein, *Angew. Chem. Int. Ed.* **1994**, *33*, 317–319.
- [10] For related Pt(II) complexes see: a) C. Mitzenheim, T. Braun, R. Laubenstein, B. Braun, R. Herrmann, *Dalton Trans.* **2016**, *45*, 6394–6404; b) J. C. DeMott, W. Gu, B. J. McCulloch, D. E. Herbert, M. D. Goshert, J. R. Walensky, J. Zhou, O. V. Ozerov, *Organometallics* **2015**, *34*, 3930–3933; c) D. Chan, S. B. Duckett, S. L. Heath, I. G. Khazal, R. N. Perutz, S. Sabo-Etienne, P. L. Timmins, *Organometallics* **2004**, *23*, 5744–5756.
- [11] The elemental analysis of complex **2.1a** shows that CH₂Cl₂ is not present, indicating that coordination of this solvent molecule is weak.
- [12] Although this compound might arise from a formal C–H coupling process instead of the C–Si route, we cannot discard the possibility that formation of complex **4.3b** from partial hydrogenation of the starting cyclometallated complex **1.3** (due to the presence of adventitious water in the reaction media able to generate H₂ in the presence of the silane) leading to the hydride [Pt(H)(IMes*)₂][BAR^F], **3.3** and subsequent reaction with ⁿBuSiH₃, releasing H₂.
- [13] a) M. Brookhart, M. L. H. Green, G. Parkin, *Proc. Natl. Acad. Sci. USA* **2007**, *104*, 6908–6914; b) G. J. Kubas in *Metal Dihydrogen and σ-Bond Complexes*, Kluwer Academic/Plenum Publishers, New York, **2001**.
- [14] M. A. Ortuño, S. Conejero, A. Lledós, *Beilstein J. Org. Chem.* **2013**, *9*, 1352–1382.
- [15] A. Sevy, E. Tieu, M. D. Morse, *J. Chem. Phys.* **2018**, *149*, 174307.
- [16] Note that two different depictions have been used to represent the interaction of the Si–H bond with the platinum center, with either a half-arrow for complex **1.3-HSiH₂ⁿBu** or a full-arrow for intermediate **A**. The purpose of this is to emphasize that in the first case the interaction takes place predominantly through the H atom (η¹-SiH coordination mode) whereas in the former the interaction occurs mainly through both the H and Si atom (η²-SiH coordination mode), according to DFT calculations, following the recommendations reported by Parkin and Green: J. C. Green, M. L. H. Green, G. Parkin, *Chem. Commun.* **2012**, *48*, 11481–11503.
- [17] R. N. Perutz, S. Sabo-Etienne, *Angew. Chem. Int. Ed.* **2007**, *46*, 2578–2592.
- [18] O. Rivada-Wheelaghan, M. Roselló-Merino, M. A. Ortuño, P. Vidossich, E. Gutiérrez-Puebla, A. Lledós, S. Conejero, *Inorg. Chem.* **2014**, *53*, 4257–4268.
- [19] a) N. Marzari, A. A. Mostofi, J. R. Yates, I. Souza, D. Vanderbilt, *Rev. Mod. Phys.* **2012**, *84*, 1419–1475; b) P. Vidossich, A. Lledós, *Dalton Trans.* **2014**, *43*, 11145–11151; c) G. Knizia, J. E. M. N. Klein, *Angew. Chem. Int. Ed.* **2015**, *54*, 5518–5522; d) P. Vidossich, A. Lledós, *ChemTexts* **2017**, *3*, 17.
- [20] a) L. Casarrubios, M. A. Esteruelas, C. Larramona, A. Lledós, J. G. Muntaner, E. Oñate, M. A. Ortuño, M. A. Sierra *Chem. Eur. J.* **2015**, *21*, 16781–16785; b) P. Villuendas, S. Ruiz, P. Vidossich, A. Lledós, E. P. Urriolabeitia, *Chem. Eur. J.* **2018**, *24*, 13124–13135; c) A. Cabré, G. Sciortino, G. Ujaque, X. Verdaguer, A. Lledós, A. Riera, *Org. Lett.* **2018**, *20*, 5747–5751.
- [21] a) F. Alber, G. Folkers, P. Carloni, *J. Phys. Chem. B* **1999**, *103*, 6121–6126; b) H. Abu-Farsakh, A. Qteish, *Phys. Rev. B* **2007**, *75*, 085201.
- [22] D. H. Binh, M. Milovanovic, J. Puertes-Mico, M. Hamdaoui, S. D. Zaric, J.-P. Djukic, *Chem. Eur. J.* **2017**, *23*, 17058–17069.
- [23] a) L. Brammer, J. M. Charnock, P. L. Goggin, R. J. Goodfellow, A. G. Orpen, T. F. Koetzle, *J. Chem. Soc., Dalton Trans.* **1991**, 1789–1798; b) P. Vidossich, M. A. Ortuño, G. Ujaque, A. Lledós, *ChemPhysChem*, **2011**, *12*, 1666–1668; c) R. Sánchez-de-Armas, M. S. G. Ahlquist, *Phys.Chem.Chem.Phys.* **2015**, *17*, 812–816.
- [24] S. Rizzato, J. Bergès, S. A. Mason, A. Albinati, J. Kozelka, *Angew. Chem. Int. Ed.* **2010**, *49*, 7440–7443.
- [25] P. Vidossich, G. Ujaque, A. Lledós, *Chem. Commun.* **2012**, *48*, 1979–1981.

FULL PAPER

Pablo Ríos, Hugo Fouilloux, Josefina Díez, Pietro Vidossich, Agustí Lledós* and Salvador Conejero*

Page No. – Page No.
 σ -Silane Platinum(II) Complexes as Intermediates in C–Si Bond Coupling Processes



Text for Table

of Contents

WILEY-VCH